Study on Autonomous Search for Multiple Radioactive Leakage Sources based on updated Infotaxis in Nuclear Emergency Rescue

Huidi Li[a,b,c], Chunhua Chen[c], Yongzhe Zheng[b*], Liwei Chen[d] , Feng Zou[a]

[a]School of Physics and Electronic Information, Huaibei Normal University, Huaibei, Anhui, 235000, China

[b]State Key Laboratory of Nuclear Power Safety Technology and Equipment, China Nuclear Power Engineering Co., Ltd., Shenzhen, Guangdong, 518172, China

[c]Institute of Nuclear Energy Safety Technology, Hefei Institutes of Physical Science, Chinese Academy of Sciences, Hefei 230031, China

[d]School of Computer Science and Technology, Hefei Normal University, Hefei, Anhui, 230601, China

Corresponding Author: 469552578@qq.com

Abstract

Nuclear facilities may experience leakage accidents due to natural, human, or war factors. Major accidents often lead to multiple leaks and form multi-source superimposed radiation fields. Accurately estimating the characteristics of leakage sources (such as time, location, type, and intensity) is crucial for emergency rescue. A multi-source radiation leakage inversion model is developed based on the updated infotaxis algorithm, considering the information entropy of superimposed radiation fields. The search path of the movement detector is optimized by adding move strategy activation function to modify next move position. Simulation results show that the hexagonal path unit improves search efficiency by 21.78% compared to the traditional quadrilateral path unit. In a scenario with three radioactive leakage sources, the mobile detector successfully identifies all source locations by traversing all grid points, with an average positioning error of 5.73m. This approach offers a new perspective for identifying multiple radioactive leakage sources in nuclear accidents.

Keywords: Nuclear emergency rescue; Multi-source search; Radioactive leakage sources; Autonomous Search

1. Introduction

With the wide application of nuclear power and radioisotopes, nuclear safety issues have emerged, such as the accidents at Three Mile Island in the United States, Chernobyl in the former Soviet Union, and the leakage of the Fukushima nuclear power plant in Japan[1]-[4]. These incidents drew public attention to nuclear safety and prompted stronger regulations and response measures[5]. Source term inversion for nuclear accidents, a vital component of emergency rescue is primarily categorized into two methods. One method is the reverse inversion technique using static sensor networks[6],[7], which collects concentration data of leaked substances from ground-based sensors. This collected information is then used in a forward diffusion model to estimate source term parameters. The second method is the mobile sensor-based source term inversion method, which uses mobile devices equipped with relevant sensors, such as robots[8]and drones[9]. The mobile device identifies the target area through rapid prediction results, and moves within the target area, collecting concentration information as it moves towards the location of the leak source, and ultimately estimate the characteristics of source. Due to the space-time and cost constraints of static sensors and the difficulty of covering all important areas[10], the more flexible and less costly mobile sensor source term inversion methods[11] are preferred in emergency rescue.

Mobile sensor source term inversion is widely applied in fields such as atmospheric science, chemical engineering, and nuclear energy, etc. Minkyu Park et al.[12] proposed a coordinated approach at different levels for information-driven source search and estimation in stochastic and turbulent atmospheric dispersion events. Yong Zhao et al.[11] proposed Entrotaxis-Jump algorithm for hazardous gas inversion in chemical production safety accidents by combining Entrotaxis algorithm and intermittent search strategy for chemical park scenario characteristics. Yuli Zhang et al.[13] proposed a collaborative search strategy based on a swarm of mobile robots with virtual physical force in order to track chemical agents accidentally or intentionally released into the environment. Cheng Zhang et al.[14] fused a particle filtering algorithm and an artificial potential field method on a single unmanned system to achieve a progressive search for unknown radioactive sources. Jianwen Huo et al.[15] proposed a multi-robot radioactive source search algorithm with distributed parameter estimation, combining artificial potential field and information entropy, and adopting a multi-robot variable step-size distributed search strategy. Tianbao Zhang et al.[16]

proposed a multiple mobile nodes cooperative search method for radioactive sources based on the navigator model. Liwei Chen et al.[17] considered radioactive decay and wet settlement caused by highpressure sprinkling or precipitation during nuclear accidents, and inverted radioactive leakage source based on the infotaxis algorithm. However, existing methods for radioactive leakage source inversion primarily focus on single-source scenarios and exhibit significant limitations when applied to multi-source cases. In multi-source superimposed fields, the concentration distribution of radioactive materials is influenced by turbulent diffusion and source superposition effects, often resulting in reduced information acquisition efficiency[18] of mobile detectors and even failures in accurately locating the leakage sources.

To address these issues, this study focuses on the complexity and challenges of multi-source leakage scenarios and proposes an autonomous search technology for multiple radioactive leakage sources tailored to nuclear emergency response efforts. This paper assumes a scenario of multiple radioactive residues present on the outside of the containment vessel in Chapter 2; Chapter 3 describes the methodology for autonomous search of multiple radioactive leakage sources: a superposition field of multiple radioactive leakage sources based on a turbulent diffusion model [19], the updated infotaxis algorithm, and a hexagonal search path unit for moving detectors[20],[21]; Chapter 4 demonstrates the method's feasibility, providing the possibility of autonomous search for multiple radioactive leak sources by a single mobile detector in nuclear emergency rescue; Chapter 5 tests a scenario involving three radioactive leakage sources within the multi-source superposition field.

2. Scenario hypothesis

In the context of nuclear accident emergency response, it is assumed that multiple leaks occur in the penetration pipelines of the containment vessel[22],[23]. These leakage points may be located at penetrations of main steam and main feedwater pipelines, high-energy pipelines, or standard fluid pipelines, among other locations. The release[24] of radioactive substances from multiple leakage points, driven by turbulent diffusion, forms a complex multi-source superimposed field, as shown in Fig 1. This results in nonlinear variations in the concentration gradients of radioactive aerosols, thereby increasing the difficulty of locating the leakage sources.

To address this scenario, a mobile detector[14] is first employed to perform spatial sampling and

localization of radioactive aerosols. The detector integrates concentration gradients and turbulent diffusion models, utilizing an infotaxis algorithm to iteratively optimize its movement path while dynamically updating the information entropy distribution to narrow down the regions of potential leakage sources. Concurrently, the detector analyzes real-time concentration data to provide directional guidance, offering precise localization references for rescue personnel. Upon identifying the location of the first leakage point, rescue personnel promptly deploy a high-altitude spray suppression system. This system typically comprises specialized nuclear decontamination vehicles, employing sealing materials such as rapid-setting concrete, epoxy resin[25], or specialized radioactive shielding materials[26] to quickly seal the leakage point and suppress further dispersion of radioactive substances. After sealing, the detector resamples the concentration distribution of the superimposed field and updates the probabilistic model to exclude the influence of treated areas, thereby improving the efficiency and accuracy of subsequent searches.

The detector then proceeds to locate the second leakage source within the updated superimposed field and applies the same high-altitude spray suppression method. This process is iteratively repeated until all leakage sources are located and sealed. By coordinating the efforts of the detector and the high-altitude spray suppression system, this emergency response strategy enables the rapid and efficient mitigation of multi-source leaks, significantly reducing the risk of radioactive substance dispersion and providing reliable technical support for rescue operations. This study assumes that radioactive leakage sources are of point-source type, with radionuclide dispersion influenced by turbulent diffusion and stable wind conditions, and further assumes that air is incompressible under room-temperature conditions.

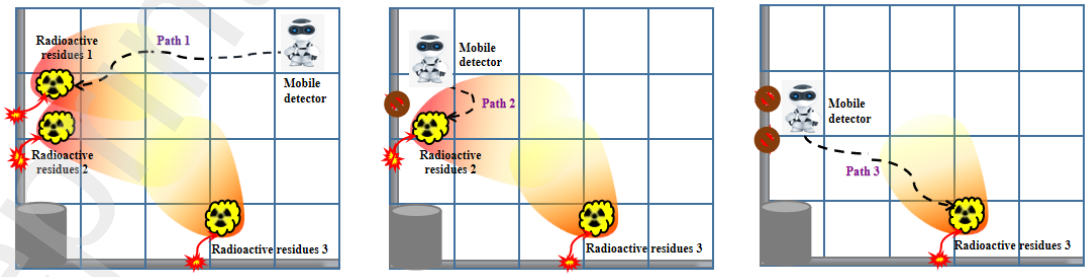

Fig. 1 Description of scenario hypothesis

3. Methodology

The autonomous search method for radioactive leakage sources in the atmosphere mentioned

in this paper mainly consists of two parts: posterior probability modelling and autonomous search strategy. Posterior probability modelling is a statistical method based on Bayesian theory, which contains three aspects, namely turbulent diffusion model, sampling rate updating, and posterior probability estimation. This approach aims to dynamically update the probability distributions of radioactive leakage source locations by continuously acquiring and analyzing new data. The autonomous search strategy guides the mobile detector's actions through two main components: the information entropy strategy and the movement control strategy. This approach optimizes the detector's path and measurement positions for efficient localization of radioactive leakage sources, as shown in Fig. 2. Step 1: Known quantity of locations of radioactive leakage sources; Step 2: Collect data and divide the grid to construct a multi-source superposition field; Step 3: Update the particle sampling rate of the corresponding grid, calculate the entropy and the entropy drop of each sample, then select the next position for the mobile detector; Step 4: Entropy Counter Decision. The entropy counter accumulates the occurrences of low radioactive residue concentrations (approaching 0) in the multi-source superimposed field. If the entropy counter reaches the preset threshold of 605, the mobile detector terminates the search. This threshold is based on the average time step during the search process and is applicable to scenarios with fewer than three radioactive leakage sources, to prevent prolonged search by the mobile detector; Step 5: Determine if a radioactive leakage source has been identified. If detected, increment the radioactive source location count; if not, return to Step 3; Step 6: Evaluate whether the termination conditions are met based on the quantity of detected locations of the leakage source and elapsed search time; Step 7: Output the quantity n of locations of the radioactive leakage source.

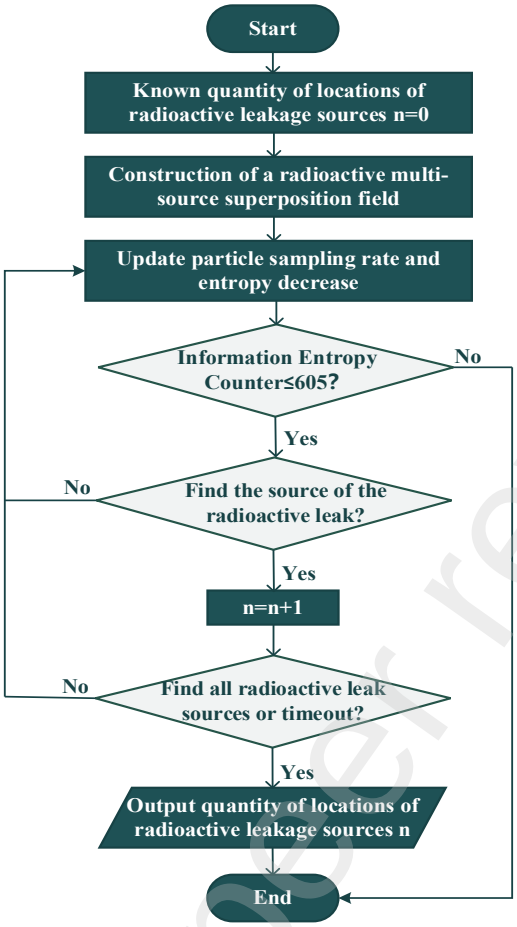

Fig. 2 Simulation flow for radioactive leakage sources location identification

3.1. Posterior probability modelling

3.1.1. Turbulent diffusion modelling

The turbulent diffusion model is a mathematical model that describes the behaviour of pollutants such as radionuclides in the atmosphere. It takes into account the effect of atmospheric turbulence on the diffusion of radionuclides and can accurately simulate their spatial and temporal distribution. The case of stable ambient wind is discussed here, assuming that the wind direction is along the negative half-axis of the y-axis, and the diffusion of radionuclides can be expressed by the following advection diffusion equation[27] :

$$0 = V\nabla_y C(r \mid r_0) + \Gamma \Delta C(r \mid r_0) - \frac{1}{\tau} C(r \mid r_0) + Q\delta(r - r_0) \tag{3.2}$$

where V is the mean wind velocity, $c(r|r_0)$ is the radionuclide concentration at position r when the radioactive leakage source is located at r_0 , Γ is the diffusion coefficient, τ is the radioactive particle lifetime, Q is the intensity of the source term at position r_0 , and δ is the impulse function.

In two dimensions, the turbulent diffusion model mean stationary concentration field can be obtained analytically from Eq. (3.1) as[19] :

$$C(r \mid r_0) = \frac{Q}{2\pi\Gamma} e^{\frac{-(y-y_0)V}{2\Gamma}} K_0(\frac{|r-r_0|}{\lambda}); \quad \lambda = \sqrt{\frac{\Gamma\tau}{1+\frac{V^2\tau}{4\Gamma}}} \tag{3.3}$$

where K_0 is the modified zero-order Bessel function, $|r - r_0|$ is the linear distance between the mobile detector and the source of the radioactive leakage, and λ is the characteristic length, which represents the average path length of a radionuclide from the source of a radioactive leak to its eventual dissipation.

3.1.2. Sampling rate updating

The sampling rate update is mainly based on the current posterior probability distribution and the latest collected data, and dynamically adjusts the sampling frequency and position selection strategy of the mobile detector to ensure that the mobile detector is able to maximise the information gain during the search process. From the classical Smoluchowski expression[27], the encounter rate between a spherical particle with radius a and a molecule with effective diffusion coefficient Γ is:

$$J(r) = 4\pi\Gamma ac(r) \tag{3.4}$$

where c(r) refers to the local particle concentration. If the detection time is T, the average of the detection events is TJ(r).

The turbulent diffusion model regards particle collisions as capturing information, and describe the spatial distribution of the information by collision probabilities. The capture rate $R(r|r_0)$ of the motion detector at position r for a radioactive leakage source at $r_0=(x_0,y_0)$ is[28] :

$$R(r \mid r_0) = \frac{2\pi\Gamma C(r \mid r_0)}{\ln(\frac{\lambda}{a})} = \frac{Q}{\ln(\frac{\lambda}{a})} e^{\frac{-(y-y_0)V}{2\Gamma}} K_0(\frac{|r-r_0|}{\lambda}) \tag{3.5}$$

3.1.3. Posterior probability estimation

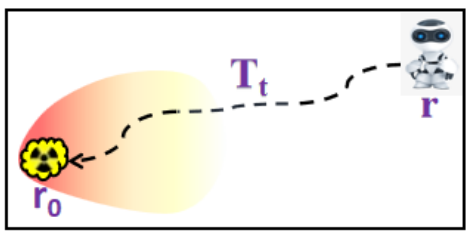

Fig. 3 Radioactive leakage source inversion process

As shown in Fig. 3, during the search for the source of radioactive leakage, the mobile detector r gradually collects information about the location of the source r_0 of radioactive leakage along its search trajectory T_t . The probability of having a trajectory T_t for a radioactive leakage source located at r_0 is:

$$L_{r_0}(T_t) = \exp[-\int_0^t R(r(t^{'}) \mid r_0)dt^{'}]\prod_{i=1}^{H} R(r(t_i) \mid r_0) \tag{3.6}$$

where H is the number of times the mobile detector detected radionuclides along the trajectory and t_i is the corresponding time.

The posterior probability distribution combines prior knowledge and posterior probability to update the estimate of the location and intensity of the source of a radioactive leak. From the Bayesian formula, the posterior probability distribution can be derived as[17] :

$$P_t(r_0) = \frac{L_{r_0}(T_t)}{\int L_x(T_t)dx} = \frac{\exp[-\int_0^t R(r(t^{'}) \mid r_0)dt^{'}]\prod_{i=1}^{H} R(r(t_i) \mid r_0)}{\int \exp[-\int_0^t R(r(t^{'}) \mid x)dt^{'}]\prod_{i=1}^{H} R(r(t_i) \mid x)dx} \tag{3.7}$$

It should be noted that $P_{t+\Delta t}(r_0)$ is determined by multiplying $P_t(r_0)$ by a factor that depends on the number of hits received in the time interval Δt. Thus the probability map is updated without tracking the entire trajectory and search history:

$$P_{t+\Delta t}(r_0) = \frac{P_t(r_0)\exp(-R(r(t+\Delta t) \mid r_0)\Delta t)R^N(r(t+\Delta t) \mid r_0)\Delta t)}{Z_{t+\Delta t}} \tag{3.8}$$

where N is the number of detector samples (hits) in the Δt time interval and $Z_{t+\Delta t}$ is the normalisation constant of $P_{t+\Delta t}$.

3.2. Autonomous search strategy

3.2.1. Information trend strategy

The infotaxis algorithm utilizes Shannon entropy as a quantitative metric to characterize the uncertainty in the probability distribution of radioactive leakage source locations. As the position of the leakage source becomes increasingly precise, the system's uncertainty progressively diminishes, with the Shannon entropy ultimately approaching zero. This reflects the process of information convergence during the localization of the leakage source. The expected entropy gain

when the mobile detector is moved is[20] :

$$\Delta S_{i\to j} = S(i) - S(i \mid j) \tag{3.9}$$

Where: the Shannon entropy is calculated as $S = -\sum_{x} p(x)\log_2 p(x)$, denoting the information gain in the current state, and S(i|j) the entropy at state i when action j is taken.

3.2.2. Decision-making for mobile control

The mobile detector refers to the possible next location points as a path unit when it is at its current position. The mobile detector will choose the optimal path unit to move based on the currently known information entropy, and the difference in the path unit will affect the performance of the infotaxis algorithm. The expected change in the entropy of its posterior probability[21] after the mobile detector moves from r_i to position r_j is:

$$\overline{\Delta S}(r_i \to r_j) = P_t(r_j)[-S] + [1 - P_t(r_j)][\rho_0(r_j)\ \Delta S_0 + \rho_1(r_j)\Delta S_1 + ...] \tag{3.10}$$

The first term on the right side corresponds to the entropy drop if the source is found after the move, while the second term corresponds to the alternative case if the source is not found at r_j . Accordingly, the mobile detector moves in the form ($\Delta S > 0$):

$$f(\Delta S_1, \Delta S_2, ..., \Delta S_i) = \arg\max(\Delta S) \quad i = 1, 2, 3...N \tag{3.11}$$

Due to the interference of multi-source, the moving strategy with the current entropy drop may face the problem of $\Delta S<0$, and it is impossible to determine the next moving point. To address this issue, this study introduces an activation function based on Eq. (3.11) to optimize the selection of the next movement position:

$$\begin{aligned} &f(\Delta S_1, \Delta S_2, ..., \Delta S_i) = u(\Delta S)\arg\max(\Delta S) + g(\Delta S_1, \Delta S_2, ..., \Delta S_i)\ ,\ u(\Delta S)\begin{cases} 1 & \exists \Delta S > 0 \\ 0 & otherwise \end{cases} \\ &g(\Delta S_1, \Delta S_2, ..., \Delta S_i) = \begin{cases} 0 & , \quad \exists : \Delta S > 0 \\ \arg\min(|\Delta S|), & \forall : \Delta S < 0 \quad i = 1, 2, 3...N \\ \Delta S_{first} & , \quad otherwise \end{cases} \end{aligned} \tag{3.12}$$

If there is a positive entropy drop, the direction with the largest positive entropy drop is selected; if all entropy drops are negative, a direction with the smallest deviation, i.e., the direction with the smallest absolute value, is selected; if the above conditions are not met, the first valid position is selected by default as the moving direction. In this study, the hexagonal search path unit

is chosen, there are six possible movement scenarios for moving the detector in the two-dimensional plane: up, down, left, right, down-left, and up-right.

4. Analysis of the effectiveness and accuracy of the algorithm

Radioactive leaks in nuclear accidents are usually not from a single source, but from multiple potential leak sources. Therefore, constructing a superposition field of multiple radioactive leakage sources is the key to emergency rescue. Due to the hazardous nature of radiation, the proposed method is difficult to be experimentally verified. This paper is based on the well-established theory of turbulent diffusion to simulate and verify the distribution of radioactive materials.

The dispersion of radionuclides in the atmosphere shares characteristics with other air pollutants, such as sulfur dioxide and nitrogen oxides. Path optimization using the infotaxis algorithm has been extensively developed and validated across various engineering fields. Sidan Deng et al.[20] compared the effects of quadrilateral, modified quadrilateral, hexagonal, and eight-point path units in atmospheric turbulence models on the performance of infotaxis algorithms. Siqi Zhang et al.[21] compared the effects of quadrilateral and hexagonal path cells on the performance of infotaxis algorithms in sparse environments, demonstrating the feasibility of path optimization for mobile detectors. This paper demonstrates the significant advantages of hexagonal path cells over traditional quadrilateral path cells through simulation-validated comparisons in a superposition field with multiple radioactive leakage sources.

5. Simulation

5.1. Analogue configuration

Before the simulation, preparatory work is outlined. This paper is based on the work of Vergassola[27] on the Python 3.7 platform, with the addition and compilation of three modules: radioactive leakage sources superposition field, information entropy counter, and hexagonal search direction for a moving detector. This work simulates a 2000m×1000m area with uniform meshing using approximately 20,000 meshes. The superposition field of radioactive leakage sources is generated by traversing the radiation fields from each source and accumulating concentration values at corresponding grid points. Finally, integrated information from multiple sources through

turbulent diffusion modelling.

The research found that the main radionuclide of multiple fission products in the fuel[29] is the volatile ^{131}I, which has a half-life of 8 days, so the dose conversion factor and radioactive decay factor of ^{131}I were chosen to be 1.6×10^{-14} and 8.02d, respectively. Sampling of radioactive aerosols by searching through the gamma detector, moving the detector at a speed of 5m • s^{-1} . Considering the early stages of the accident, the maximum of each radioactive leakage source's search time of 3600s is considered as a search failure, and the time step is set to 1s. The wind speed is 1 m • s^{-1} , the diffusion coefficient of radionuclides in the atmospheric environment is 50 m^2 • s^{-1} , and the maximum positioning error to be 10 m. Assuming that the three continuous stable radioactive leakage sources of ^{131}I are located at the coordinates (300, 300), (320, 320), and (380, 380), indicated by the black pentagrams, corresponding to a radiative leakage source intensity of 2 kBq • s^{-1}, 5 kBq • s^{-1}, and 8 kBq • s^{-1}, respectively. The starting point of the mobile detector is at (1900, 900), indicated by a brown dot. The simulated distribution of the multi-source superimposed environment is shown in Fig. 4, which exhibits the distribution of ^{131}I in the atmospheric environment under the conditions of a leakage accident, where red and blue colors indicate the maximum and minimum values of ^{131}I concentration, respectively.

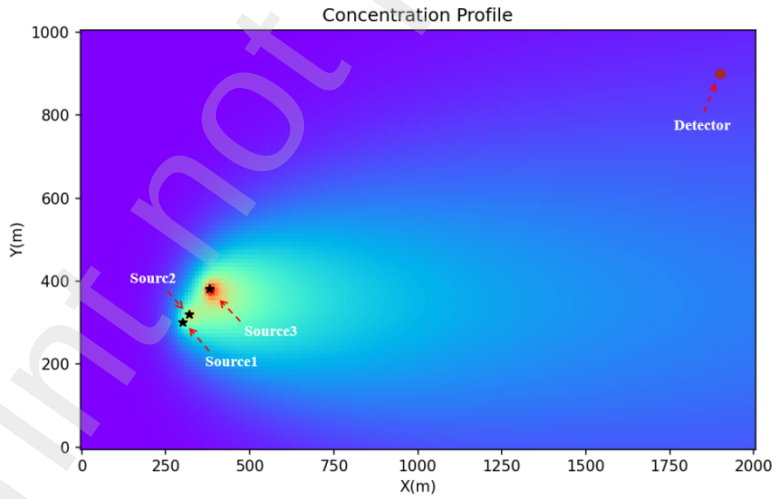

Fig. 4 Radioactive multi-source superposition field.

5.2. Results and Discussion

5.2.1. Multi-source autonomous localization search

Fig. 5 shows the trajectory of the first stage of motion of the mobile detector generated based

on the radioactive superposition field. Fig. 5(a) shows the radioactive superposition field for Q_1=2kBq • s^{-1}, Q_2=5kBq • s^{-1}, and Q_3=8kBq • s^{-1}, Q_3 has the largest intensity, the widest distribution, and the closest color to red. Fig. 5(a) to 5(f) show the inversion process for a radioactive leakage source Q_3=8kBq • s^{-1} based on the distribution of the radioactive plume profile at 6 time intervals by the mobile detector from the starting position (1900,900), sampling the radioactive aerosol and moving according to the activation function of the mobile strategy.

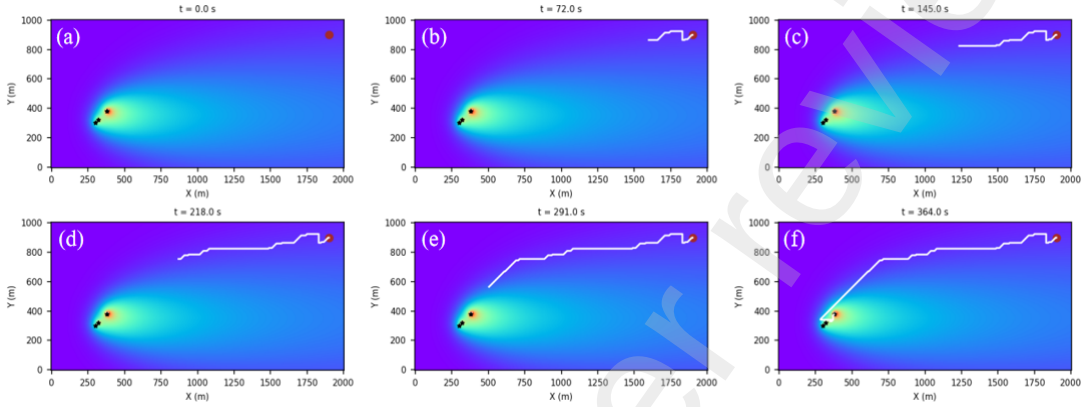

Fig. 5 Trajectories of the first stage of the moving detector at Q_1=2kBq • s^{-1}, Q_2=5kBq • s^{-1}, and Q_3=8kBq • s^{-1}. (a) t = 0 s; (b) t = 72 s; (c) t = 145 s; (d) t = 218 s; (e) t = 291 s; (f) t = 364 s.

The simulation results show that the mobile detector detects the radioactive leakage source Q_3 located at (375,375), and there is a positioning error of about 7.07m. At the current location, the mobile detector implements measures such as blocking, dilution or isolation to suppress the radioactive leakage source of Q_3=8kBq • s^{-1} by means of a robotic arm or a spraying device, which effectively reduces the spread of radioactive material[25],[26]. Afterwards, update the sampling probability map and move detector to start at (375,375), based on the moving strategy activation function. The grid cell where the second radioactive leakage source Q_2=5kBq • s^{-1} is located is identified and suppressed, and the time step used to search for the second source of radioactive leakage, and the positioning coordinates are outputted. Iterate sequentially to complete the third stage of the source term inversion.

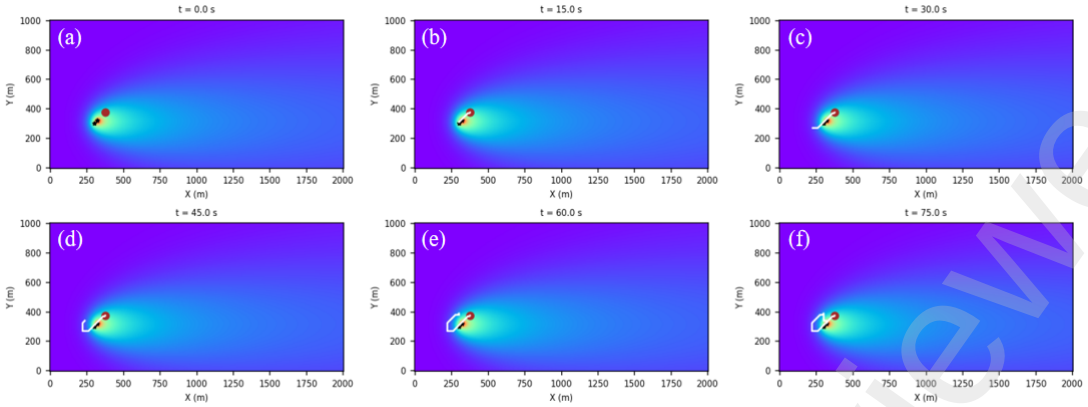

Fig. 6 Trajectories of the second stage of the moving detector at Q_1=2kBq • s^{-1}, Q_2=5kBq • s^{-1}, and Q_3=8kBq • s^{-1}. (a) t = 0 s; (b) t = 15 s; (c) t = 30 s; (d) t = 45 s; (e) t = 60 s; (f) t = 75 s.

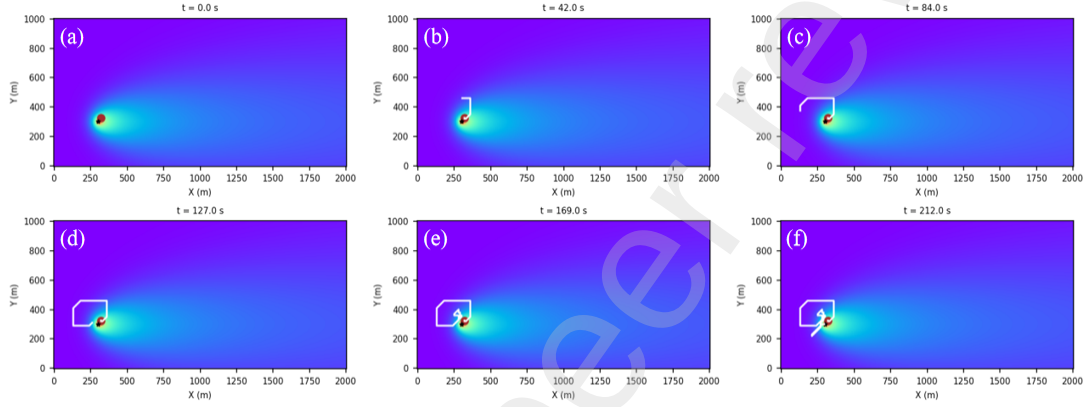

Fig. 7 Trajectories of the third stage of the moving detector at Q_1=2kBq • s^{-1}, Q_2=5kBq • s^{-1}, and Q_3=8kBq • s^{-1}. (a) t = 0 s; (b) t = 42 s; (c) t = 84 s; (d) t = 127 s; (e) t = 169 s; (f) t = 212 s.

Fig. 6 and Fig. 7 show the trajectories of the mobile detector during the second and third phases, respectively, from which it can be seen that the mobile detector locates the radioactive leakage sources of Q_2=5kBq • s^{-1} and Q_1=2kBq • s^{-1} in turn. The simulation shows that Q_2 is located at (320,325) with about 5m positioning error and Q_1 is located at (295,300) with about 5m positioning error. Considering the different levels of nuclear leakage accidents, three variables, namely the intensity of the radioactive leakage sources, the locations of the radioactive leakage sources, and the starting point of the mobile detector's search, were chosen to observe the inversion effect of the radioactive leakage sources. The results are presented in Tables 1, 2, and 3. Table 1 corresponds to the intensity of the different radioactive leakage sources, with the difference in intensity of the three radioactive leakage sources increasing row by row. Table 2 corresponds to the locations of the different radioactive leakage sources, and the distances of the three radioactive leakage sources are 20-50m, 50-100m and 100-500m, respectively. Table 3 corresponds to the different mobile detector search starting points, the three search starting points correspond to the lower left, upper left and upper right corners of the search area.

Table 1 Test data for different intensities

Source1 intensity Q_1(kBq·s^{-1})	Source2 intensity Q_2(kBq·s^{-1})	Source3 intensity Q_3(kBq·s^{-1})	Start position	Leakage source1	Leakage source2	Leakage source3	Search time(s)
5	5	5	(1900,900)	(300,300)	(320,320)	(380,380)	697
1	3	5					856
1	5	30					3744

Table 2 Test data for different positions

Source1 intensity Q_1(kBq·s^{-1})	Source2 intensity Q_2(kBq·s^{-1})	Source3 intensity Q_3(kBq·s^{-1})	Start position	Leakage source1	Leakage source2	Leakage source3	Search time(s)
2	5	8	(1900,900)	(300,300)	(300,320)	(300,350)	649
				(300,300)	(350,300)	(400,300)	734
				(300,300)	(300,400)	(300,800)	1154

Table 3 Test data for different search starting points

Source1 intensity Q_1(kBq·s^{-1})	Source2 intensity Q_2(kBq·s^{-1})	Source3 intensity Q_3(kBq·s^{-1})	Start position	Leakage source1	Leakage source2	Leakage source3	Search time(s)
2	5	8	(10,10)	(300,300)	(320,320)	(380,380)	489
			(10,900)				1220
			(1900,900)				654

Table 1 shows that when the intensity of the three radioactive leakage sources are more different, the mobile detector needs to spend more search time, and the search time of group 3 is 2888s more than that of group 2. Table 2 shows that when the locations of the three radioactive leakage sources are farther away from each other, the mobile detector needs to spend more search time, and the search time of group 3 is 505s more than that of group 1. From Table 3, it can be seen that the starting position of the mobile detector has less influence on the search result (whether or not the radioactive leakage source can be found).Meanwhile, in order to verify the feasibility of the method, the simulation experiment traverses all the search starting points in the grid with a unit length of 10, and sets the radioactive leakage source locations (300, 300), (320, 320), (380, 380), corresponding to the intensity of the radioactive leakage source of 2kBq • s^{-1},5kBq • s^{-1},8kBq • s^{-1} . The simulation results show that the motion detectors are all able to successfully identify the locations of the three sources and have an average localization error of 5.73m.

5.2.2. Search Path Comparison

In information trend search, the current mobile detector is at a certain position and its possible next position point is referred to as a path unit. As shown in Fig. 8(a), the basic quadrilateral search path unit of the infotaxis algorithm[20] , the red circle is the current position of the mobile detector, and the white circle is the position that the mobile detector moves to next. This section comparatively analyses several different path units mentioned by previous authors, improved quadrilateral, hexagonal and eight-point, as shown in Fig. 8(b), (c) and (d).

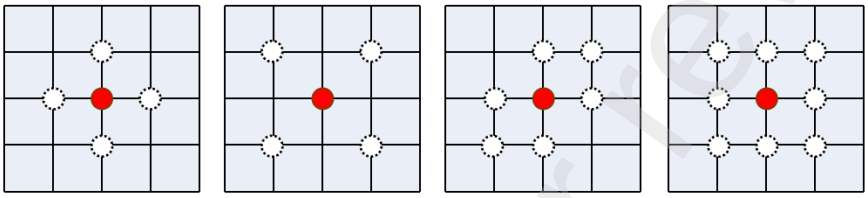

Fig. 8 Path unit

In the simulation experiment, the positions of three radioactive leakage sources are set to be (300,300), (320,320), and (380,380), and the search results under different search path units are compared by adjusting the starting position of the mobile detector as well as the intensity of the radioactive leakage sources. As shown in Table 4, the variables in the first 4 groups are the starting position of the moving detector, and the variables in groups 5 and 6 are the intensity of the radioactive leakage source. Here the case of timeout (search for a leakage source in time steps greater than 3600s) is considered as a source search failure.

Table 4 Path unit test data

Source1 intensity Q_1(kBq·s^{-1})	Source2 intensity Q_2(kBq·s^{-1})	Source3 intensity Q_3(kBq·s^{-1})	Start position	Search time(s)			
				Quadrilateral	Improved quadrilateral	Hexagon	Eight point type
2	5	8	(10,10)	622	364	489	454
2	5	8	(10,900)	1154	348	1220	266
2	5	8	(1900,10)	1124	754	654	806
2	5	8	(1900,900)	754	750	654	771
5	5	5	(600,600)	782	352	333	621
2	5	25	(600,600)	*Not found*	*Not found*	773	*Not found*
-	-	-	-	887	513	687	584

Comparing the results of radioactive leakage source search under different search path units, it

can be seen that, under the same settings of source intensity, source location, and search starting point of the mobile detector, the mobile detector chooses different search path units with different effects. From the data in groups 3, 4 and 5, it can be seen that the hexagonal path unit spends the shortest search time compared with the other three path units, which are 654s, 654s and 333s, respectively. From the 6th set of data, it can be seen that when the intensity of the radioactive leakage source is 25kBq·s^{-1} at maximum, the search time of the hexagonal path unit is 773s, and the other three path units do not find the radioactive leakage source. The four paths in the same environment are simulated, and the tests show that the hexagonal path unit improves the search efficiency by 21.78% over the original quadrilateral path unit in the infotaxis[27] algorithm, which can satisfy the searching needs of the mobile detector in the multi-source superposition field.

6. Conclusions

This study addresses the challenge of multiple radioactive leakage sources in nuclear accident rescue scenarios. By constructing a multi-source radioactive superimposed field based on a turbulence diffusion model and introducing a mobility strategy activation function, the research effectively resolves the information entropy issue and optimizes the hexagonal search path of the mobile detector. The proposed approach successfully achieves autonomous and efficient localization of multiple radioactive leakage sources, avoiding complex information transmission processes and reducing search costs, thereby offering a novel solution for source localization in multi-source leakage scenarios.

Despite these advancements, certain limitations remain, and future research can focus on the following directions for improvement: (1) Map complexity. There are only three radioactive leakage sources and one mobile detector in the current search map, and the obstacles in the actual scene are not considered. Subsequent consideration will be given to combining with the actual 3D scene to include obstacles and optimize the search path to increase feasibility. (2) Leak location. The current hypothetical scenario is a leakage of piping outside the containment vessel triggered by an external event, and the leakage source is a point source. Subsequent consideration will be given to the size of the containment and the location of the possible leak.

CRediT authorship contribution statement

Declaration of competing interest

Data availability

Acknowledgements

This work was supported by the Outstanding Talent Support Program at the University of Anhui Province (gxyq2022060), the Open Project of Anhui Intelligent Security Technology Engineering Research Center (2023ZNAJKF06). This work was partially supported by the fund from State Key Laboratory of Nuclear Power Safety Technology and Equipment (K-A2021.414). Thanks for the technical support by Institutional Center for Shared Technologies and Facilities of INEST, HFIPS, CAS.

References

[1] Löfquist L. After Fukushima: nuclear power and societal choice[J]. Journal of Risk Research, 2015, 18(3): 291-303.

[2] Nagatani K, Kiribayashi S, Okada Y, et al. Emergency response to the nuclear accident at the Fukushima Daiichi Nuclear Power Plants using mobile rescue robots[J]. Journal of Field Robotics, 2013, 30(1): 44-63.

[3] Yue H. Nuclear Accident Emergency Preparedness and Response Manual[J]. China Environmental Science Press, 2012.

[4] Abouaf J. Trial by fire: teleoperated robot targets Chernobyl[J]. IEEE Computer Graphics and Applications, 1998, 18(4): 10-14.

[5] Kun Q I, Zhang X, Shijun Q U, et al. Exploration of the construction of nuclear emergency response capability in prefecture-level cities[J]. Chinese Journal of Radiological Health, 2024, 33(5): 559-565.

[6] Brennan S M, Mielke A M, Torney D C. Radioactive source detection by sensor networks[J]. IEEE Transactions on Nuclear Science, 2005, 52(3): 813-819.

[7] Kovalets I V, Efthimiou G C, Andronopoulos S, et al. Inverse identification of unknown finite-duration air pollutant release from a point source in urban environment[J]. Atmospheric Environment, 2018, 181: 82-96.

[8] Chang F, Congzheng W, Jian** Z, et al. Research status and key technologies analysis of operating robots for nuclear environment[J]. Opto-Electronic Engineering, 2020, 47(10): 200338-1-200338-11.

[9] Cho H S, Woo T H. Mechanical analysis of flying robot for nuclear safety and security control by radiological monitoring[J]. Annals of Nuclear Energy, 2016, 94: 138-143.

[10] Hutchinson M, Oh H, Chen W H. A review of source term estimation methods for atmospheric

dispersion events using static or mobile sensors[J]. Information Fusion, 2017, 36: 130-148.
[11] Yong Z, Chen B, Wang X, et al. Research on Source Seeking Methods of Harmful Gas leakage in Chemical Industry Parks[J]. Journal of System Simulation, 2019, 31(12): 2810-2815.
[12] Park M, Oh H. Cooperative information-driven source search and estimation for multiple agents[J]. Information Fusion, 2020, 54: 72-84.
[13] Zhang Y L, Ma X P, Miao Y Z. A virtual physics-based approach to chemical source localization using mobile robots[J]. Applied Mechanics and Materials, 2013, 263: 674-679.
[14] Zhang C, **ao Y, Liu H, et al. Search method of radioactive source based on particle filter and artificial potential field[J]. Nuclear Physics Review, 2020, 37(4): 867-874.
[15] Huo Jianwen, Liu Hongwei, Ling Mingrun, et al. Multi-robot Radioactive Source Search Strategy Based on Distributed Parameter Estimation[J]. Journal of Southwest University of Science and Technology, 2023, 38(02): 85-91.
[16] ZHANG T, FAN J, DU S, et al. Source Search Method of Mobile Nodes Formation Based on Leader Model[J]. Atomic Energy Science and Technology, 2021, 55(zengkan): 136.
[17] Chen L, Zhou C, Wang Y, et al. Autonomous search investigation for radioactive leaked source based on an updated infotaxis method during nuclear emergency rescue[J]. Nuclear Engineering and Design, 2024, 416: 112769.
[18] Yan D, **ao Y, Sheng S, et al. Radioactive sources search method based on multi-robot and Voronoi partition[J]. Applied Radiation and Isotopes, 2024, 212: 111475.
[19] Song C, He Y, Yang P, et al. An infotaxis strategy for seeking a dispersion source using local probabilistic reliability[J]. Journal of Northwestern Polytechnical University, 2016: 843-850.
[20] Sidan D, Shurui F, Yan Z. Reasearch on location method of infotaxis research algorithm on gas diffusion model[J]. Electron. Meas. Technol, 2022, 45(12): 58-65.
[21] Zhang S, Cui R, Demin X U. Performance analysis on the infotaxis algorithm for searching in dilute environments[J]. Robot, 2013, 35(4): 432-438.
[22] SHAN Qiang, CHEN Yingyu, WANG Yongchao. Analysis of reasons for exceeding leakage rate in containment test and strategy for leakage detection [J]. Technology Innovation and Application, 2024, 14(02): 142-147.
[23] ZHAO Wenbin, CHEN Xiaoxia, ZHAO Danfeng, et al. Design and Research on New Mechanical Penetration in Nuclear Power Plant [J]. China Academic Journal Electronic Publishing House, 2022, (23): 262-265.
[24] Chen L, Chen C, Zheng X, et al. Simulation of radionuclide diffusion in a dry storage of spent fuel under accident condition[J]. Progress in Nuclear Energy, 2018, 108: 152-159.
[25] Yao B. Providing strong support and assurance for the realization of the chinese dream-ideas and proposals for enhancing nuclear emergency EPR work in the new era[J]. China Nuclear Power, 2019, 12(1): 7-10.
[26] Lipeng W, **uhua T, Lin L, et al. Optimization methods for nuclear accident emergencies' early off-site intervention strategy[J]. Radiation Protection (Taiyuan), 2013, 33.
[27] Vergassola M, Villermaux E, Shraiman B I. 'Infotaxis' as a strategy for searching without gradients[J]. Nature, 2007, 445(7126): 406-409.
[28] Liu S, Zhang Y, Fan S. Adaptive Space-Aware Infotaxis II as a Strategy for Odor Source Localization[J]. Entropy, 2024, 26(4): 302.
[29] Xiao D, Zhang Z, Li J, et al. Source term inversion of nuclear accidents based on ISAO-SAELM model[J]. Nuclear Engineering and Technology, 2024, 56(9): 3914-3924.